Journal of Solid Mechanics and Materials Engineering

Vol. 4, No. 3, 2010

Effect of UIT on Fatigue Life in Web-Gusset Welded Joints*

Yu TOGASAKI**, Hirokazu TSUJI***, Takashi HONDA****, Tetsuya SASAKI**** and Atsushi YAMAGUCHI****

**Graduate School of Tokyo Denki University
Ishizaka, Hatoyama, Hiki-gun, Saitama 350-0394, Japan
E-mail: togasaki@tsujilab.n.dendai.ac.jp
***Tokyo Denki University
****National Institute of Occupational Safety and Health, Japan
Umezono 1-4-6, Kiyose, Tokyo 204-0024, Japan

Abstract

Ultrasonic impact treatment (UIT), which is a peening method, is usually used as a post-weld treatment in order to improve the fatigue strength of welded joints. In this study, fatigue tests were carried out on web-gusset welded joints treated by UIT and the results were compared with the fatigue lives of as-welded joints in order to examine the effects of UIT on the fatigue lives of welded joints. The fatigue lives of web-gusset welded joints treated by UIT increased to more than ten times those of as-welded joints. The introduction of compressive residual stress, relaxation of stress concentration at a weld toe, and refinement of grains under the weld toes were considered as possible reasons for the improvement in fatigue life caused by UIT. Residual stress near weld toes was measured using the X-ray diffraction method. The stress concentration factor at the weld toes was analyzed using the finite element method (FEM). The grain size under the weld toes was measured using electron backscatter diffraction pattern (EBSD) analysis.

Key words: Welded Joint, Fatigue, Stress Concentration, Residual Stress, Grain Size

1. Introduction

Welded joints used in steel structures such as cranes and bridges are often the cause of failure accidents as a result of fatigue cracks at the weld toes initiated by the weld geometries or defects[(1)]. The fatigue lives of welded joints are much lower than those of base metals because of the tensile residual stress and stress concentration at weld toes[(2)]. The fatigue life of a web-gusset welded joint in particular needs to be improved since its fatigue life is considerably lower than that of other types of weld joints.

A reduction in the tensile residual stress and relaxation of the stress concentration at the weld toes are required to improve the fatigue lives of welded joints. Shot peening and hammer peening are used to introduce compressive residual stress in weld joints[(3)(4)]. The stress concentration of a weld toe can also be reduced using the grinder method or tungsten-inert gas (TIG) dressing[(4)(5)]. Ultrasonic impact treatment (UIT), which is a peening method that was developed in Russia, is applied to welded joints as a post-weld treatment in order to introduce compressive residual stress and relax the stress concentration at weld toes. The application of UIT to steel structures such as cranes and ships is performed as a substitute for shot peening or griding[(6)(7)]. However, there is insufficient fatigue data available on welded joints treated by UIT for it to be applied to actual steel structures.

*Received 13 Oct., 2009 (No. 09-0587)
[DOI: 10.1299/jmmp.4.391]

In this study, fatigue tests were carried out on web-gusset welded joints treated by UIT and the results were compared with the fatigue lives of as-welded joints. Also, the changes in residual stress, stress concentration factor, and grain size around the weld toes were measured after UIT was applied in order to clarify the reason for the improvement in the fatigue lives of welded joints.

2. Experimental Procedure

2.1 UIT and specimens

Figure 1 shows a schematic of a UIT system, the Applied Ultrasonic ESONIX™27 UIS. This equipment consists of a generator, a cooling unit, and a hand tool. The pins mounted on the tip of the hand tool are vibrated by ultrasonic waves generated in the transducer. The radius of curvature of the pin tip is 3 mm. The resonant frequency of the pins is 27 kHz and the amplitude of the pins is about 30 μm.

The specimens used in this study were machined from a plate of JIS SM570Q with a thickness of 12 mm. Table 1 shows the mechanical properties of the material used. Table 2 shows the chemical composition of the material used. The welding of the web gussets was carried out using the carbon dioxide semi-automatic arc welding method with YFW-C60FM (JIS Z 3313) of the weld metal. Table 3 shows the welding conditions. Figure 2 shows the configuration of the web-gusset welded joint specimens used. Half of the specimens were treated by UIT until grooves at the weld toe completely disappeared.

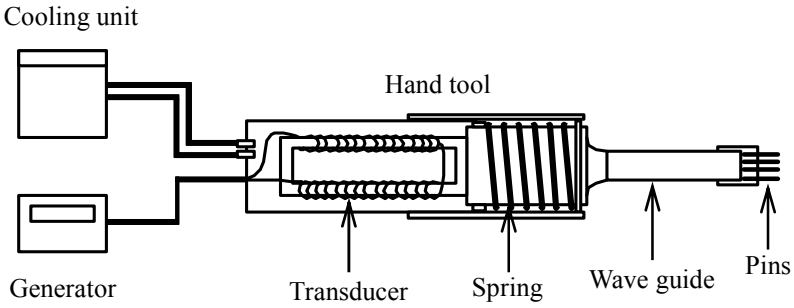

Fig. 1 Schematic of UIT system.

Table 1 Mechanical properties of material used.

	Yield strength MPa	Tensile strength MPa	Elongation %
SM570Q	514	608	34

Table 2 Chemical composition of material used. (wt. %)

	C	Si	Mn	P	S	Ni	Cr	Nb	V
SM570Q	0.11	0.23	1.53	0.007	0.002	0.02	0.02	0.02	0.06

Table 3 Welding conditions.

Current	25 A
Voltage	270 V
Welding speed	33 mm/min
Carbon dioxide flow rate	300 l/min
Leg length	10 mm

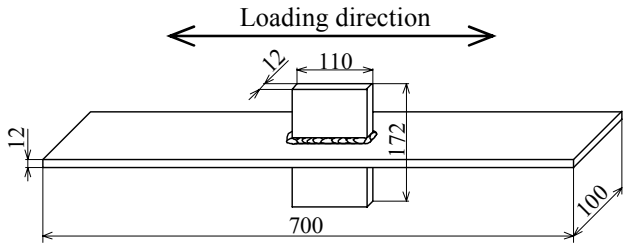

Fig. 2 Configuration of web-gusset welded joints. (unit: mm)

2.2 Fatigue test

Fatigue tests were carried out based on the 14*S-N* testing method as regulated in JSME S 002-1994, the standard method of statistical fatigue testing[8]. Fatigue tests were conducted at room temperature under a load frequency f of 4 to 9 Hz and a stress ration R of 0.1 using a servo-hydraulic fatigue machine with a capacity of 1500 kN. Fatigue tests were terminated in cases where the number of load cycles reached 10 million. During fatigue tests, the strain amplitude of each weld toe was measured with a strain gage attached at a point 5 mm from the weld toe in order to detect a fatigue crack initiated at the weld toe. The crack initiation life at a weld toe was defined as the number of cycles in which the value R_s, calculated by using Eq. (1), decreased 5%[9].

$$R_S = \frac{\varepsilon_i}{\varepsilon_0} \times 100 \tag{1}$$

where ε_i is the strain amplitude during the fatigue test and ε_0 is the value of the initial strain amplitude.

3. Results and Discussion

3.1 Fatigue test results

Figure 3 shows an *S-N* curve diagram for the UIT specimens. For comparison, the results for the as-welded (AW) specimens are also shown in this figure. The fatigue lives of web gusset welded joints were greatly improved throughout the whole stress range by the UIT. The fatigue lives of the UIT specimens were increased more than tenfold in the stress range where $\Delta\sigma$ is equal to 175 MPa or less. Also, the fatigue limit of web gusset welded joints increased from 53 MPa to 111 MPa.

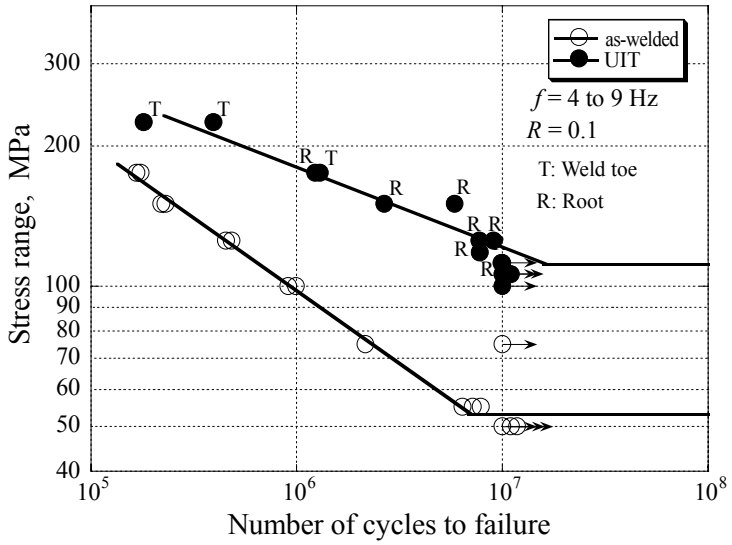

Fig. 3 Effect of UIT on fatigue life.

Although fatigue cracks were initiated at the weld toes for all the AW specimens, the locations of the fatigue cracks initiated in the UIT specimens varied according to the stress range. The locations of the fatigue cracks are indicated in Figure 3. In this figure, T indicates that a crack was initiated at a weld toe, while R indicates that a crack was initiated at a weld root. In the high stress range of over 175 MPa, a fatigue crack was initiated at the weld toe, as shown in Figure 4 (a). Meanwhile, a fatigue crack was initiated at the weld root, as shown in Figure 4 (b), in the low stress range.

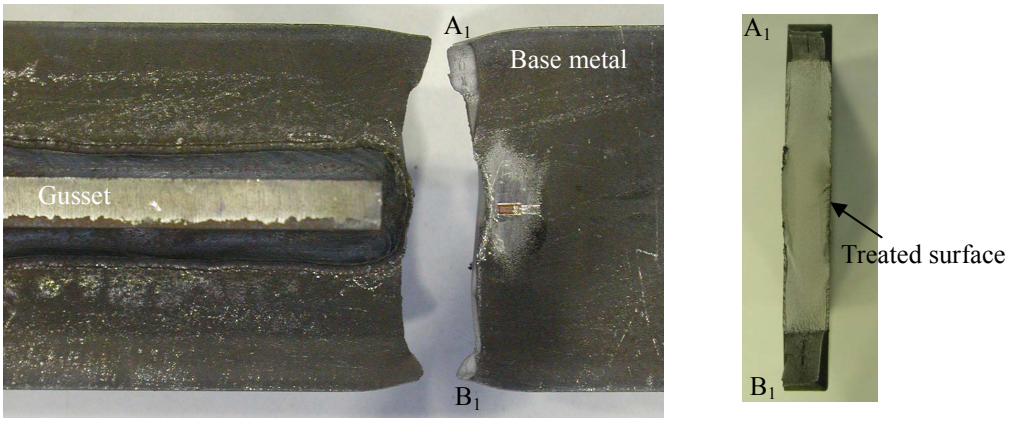

(a) High stress range

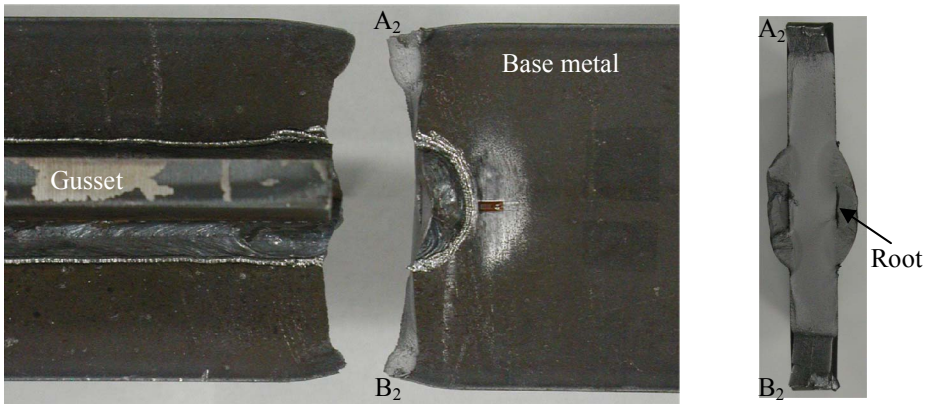

(b) Low stress range

Fig. 4 Typical examples of fatigue fractured specimens treated by UIT.

Figure 5 shows the relationship between the strain gage output and the number of cycles at a stress of 175 MPa. Cracks in both the AW specimen and the UIT specimen were initiated at the weld toes. At first, R_s remained 100% before it gradually fell after the fatigue crack was initiated. The fatigue crack initiation life N_c and the fatigue crack growth life N_f were determined based on the change in the strain gage output, R_s. Table 4 shows a comparison between the fatigue lives of the AW specimen and the UIT specimen tested at a stress of 175 MPa. The N_c of the UIT specimen was about thirty times that of the AW specimen. Meanwhile, the N_f of the AW specimen was almost equal to that of the UIT specimen. In the stress range of over 175 MPa, the improvement in the fatigue life of web-gusset welded joints applied to UIT was caused by an increase of N_c.

Figure 6 shows the relationship between the strain gage output and the number of cycles at a stress of 125 MPa. Fatigue cracks in the AW specimen were initiated at the weld toes, while fatigue cracks in the UIT specimen were initiated at the weld roots. As it is impossible to accurately determine the crack initiation life by using strain gages attached at

the weld toes because fatigue cracks in the UIT specimen were initiated at the weld roots, the fatigue crack initiation life N_c and the fatigue crack growth life N_f were determined from Figure 6. Table 5 shows a comparison between the fatigue lives of the AW specimen and the UIT specimen tested at a stress of 125 MPa. The N_c and N_f were dramatically increased. In the stress range of 175 MPa or less, the fatigue life was increased more than tenfold in cases where a crack was initiated at a weld root.

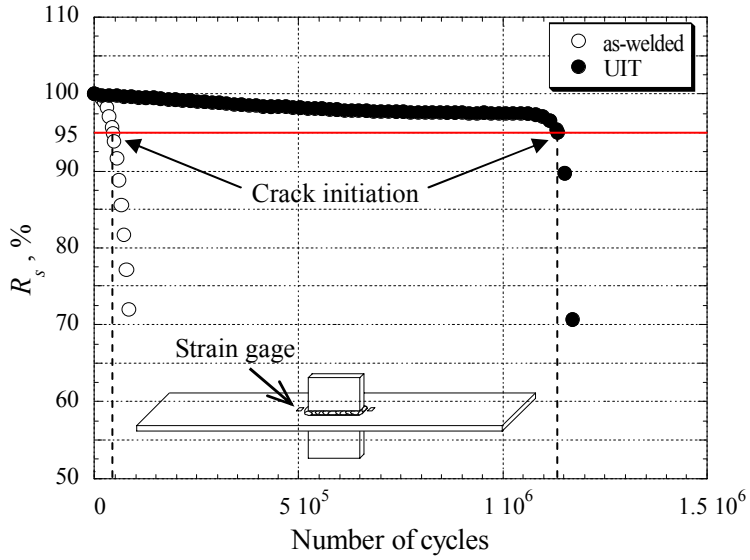

Fig. 5 Relationship between R_s and number of cycles. ($\Delta\sigma$=175 MPa)

Table 4 Comparison between fatigue lives of AW specimen and UIT Specimen. ($\Delta\sigma$=175 MPa)

	N_i cycles	N_f cycles	N_t cycles
As-weld	45,000	121,981	166,981
UIT	1,132,920	101,296	1,234,216

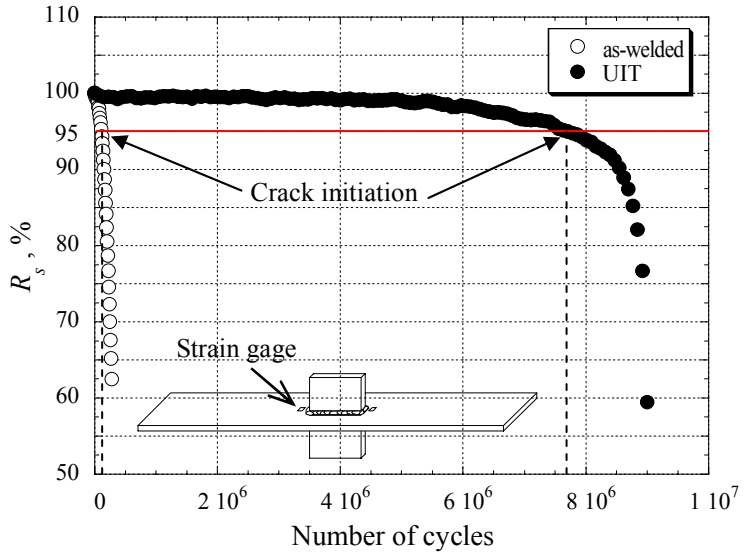

Fig. 6 Relationship between R_s and number of cycles. ($\Delta\sigma$=125 MPa)

Table 5 Comparison between fatigue lives of AW specimen and UIT Specimen. ($\Delta\sigma$=125 MPa)

	N_i cycles	N_f cycles	N_t cycles
As-weld	108,400	374,696	483,096
UIT	7,636,113	1,438,717	9,074,830

3.2 Factors affecting the fatigue lives of welded joints

3.2.1 Residual stress

The residual stress distribution on the surface along the cross section at the weld toe of the AW specimen and that of the UIT specimen were measured using an X-ray diffraction stress analyzer (Rigaku PSPC-MSF-2) with an X-ray target CrKα. The peak location of the residual stress was calculated using the half-breadth method and seven Ψ angles were used to determine the slope of $sin2\Psi$ - 2θ diagram[10]. The diffraction angle was 156.08°, and the irradiation area was 4 mm^2.

The distributions of the longitudinal residual stress, which was measured using the X-ray diffraction method, are shown in Figure 7. Although the maximum tensile residual stress was over 300 MPa at the weld toe in the AW specimen, the residual stress at the weld toe in the UIT specimen was 200 MPa compressive residual stress. The large amount of compressive residual stress, which exceeded the amount of tensile residual stress, was introduced by UIT.

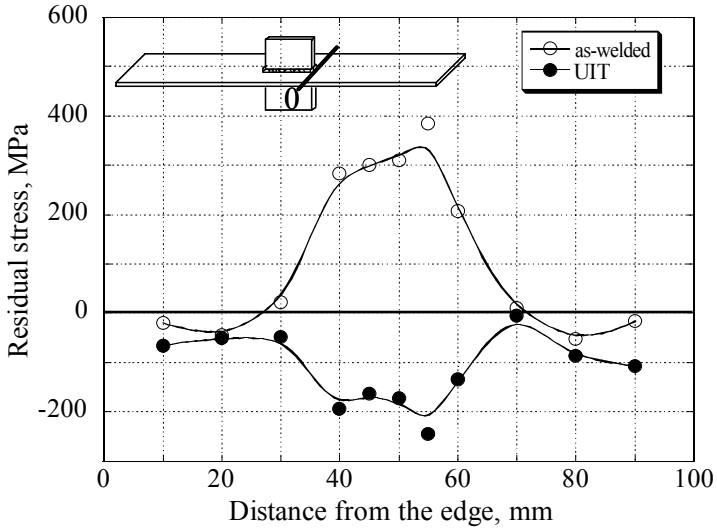

Fig. 7 Residual stress distribution.

3.2.2 Stress concentration factor

The stress concentration factor K_t at the weld toes in the AW specimen and that in the UIT specimen were calculated by performing an elastic stress analysis using the three-dimensional finite element method (FEM) code MARC. Replicas of the weld zones were made in silicone rubber. The configurations of the replicas were measured using an optical microscope with a 10x object lens. In particular, the radii of the weld toes were accurately measured using a 3-D laser microscope (KEYENCE VK-9510) with a resolution of 0.01 μm. The radii of the weld toes ρ and the flank angles θ are shown in Table 6. The radii of weld toes in UIT specimens approximately coincided with the curvature of the pin tip mounted on the hand tool in the UIT equipment. Figure 8 shows typical FE models using the measurement results for the weld zones. Given the symmetry of the specimens, one in eight FE models was meshed with 60,000 elements and 66,000 nodes using 8-node-solid-elements. Young's modulus was 206 GPa and Poisson's ratio was 0.3.

The stress contours of σ_{xx} around the weld toes are shown in Figure 9. The stress concentration is relaxed by the use of UIT. The values for K_t, which were calculated from the FEM results, are shown in Table 7. The K_t for the UIT specimens was about 40% less that that for the AW specimens.

Table 6 Comparison of weld geometry between as-welded and UIT

	Specimen No.		1	2	3	4	5
as-welded	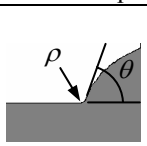	ρ mm	0.49	0.55	0.19	0.47	0.38
		θ°	58.0	62.5	55.0	54.0	64.0
UIT		ρ mm	2.30	2.30	2.30	2.50	2.50
		θ°	32.0	37.0	37.5	42.5	37.0

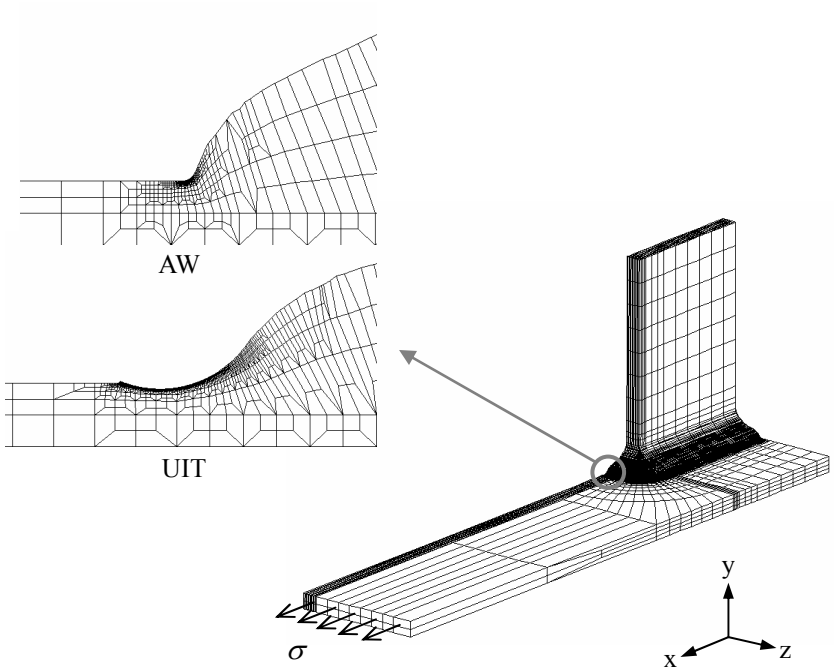

Fig. 8 Typical FE models for AW specimen and UIT specimen.

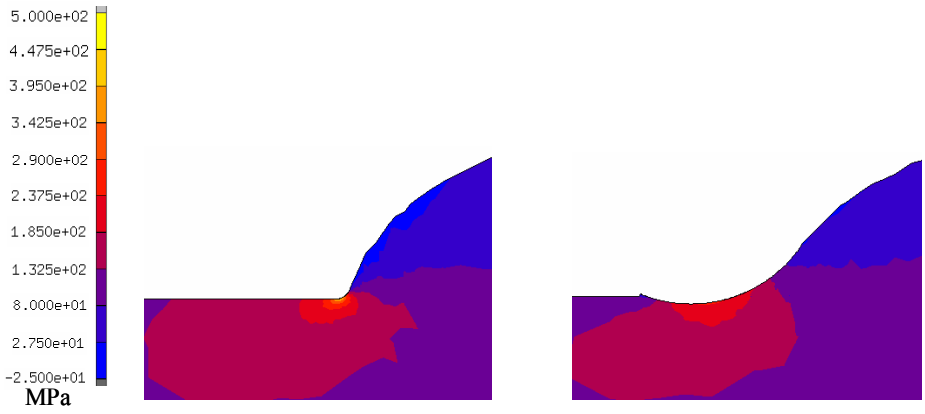

(a) AW (b) UIT

Fig. 9 Stress contours around weld toes. (σ_{xx})

Table 7 Stress concentration factors calculated using FEM.

Specimen No.	1	2	3	4	5
as-welded	4.33	4.42	5.43	4.60	4.81
UIT	2.64	2.64	2.84	2.55	2.47

3.2.3 Grain refinement

Microstructures around the weld toes etched with 2.5% Nital were observed using the laser microscope (KEYENCE VK-9510). Figure 10 shows the microstructures around the weld toes. Unlike for the AW specimen, the refinement of the grains was observed from the surface to 300 μm in depth for the UIT specimen. The grain sizes from the surface to 25 μm in depth at the weld toes were measured using electron backscatter diffraction pattern (EBSD) analysis. The grain boundary was defined as the location at which the change in the crystal orientation exceeded 15°. Also, the grain size was defined as the diameter of a circle that was equivalent to the grain in area. Figure 11 shows images of the grain boundary at the weld toes in the AW specimen and the UIT specimen. The grain sizes in the AW specimen ranged from 5 to 14 μm. Meanwhile, the grain sizes in the UIT specimen ranged from 0.3 to 0.7 μm, one-tenth or less the grain sizes in the AW specimen.

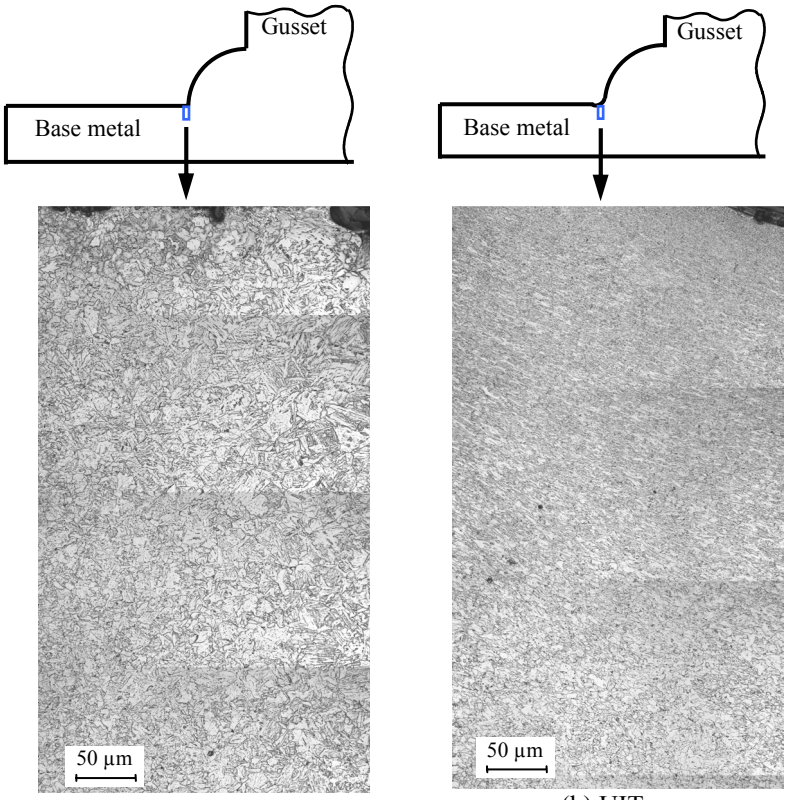

(a) AW (b) UIT

Fig. 10 Comparison between microstructures around weld toes of AW specimen and UIT specimen.

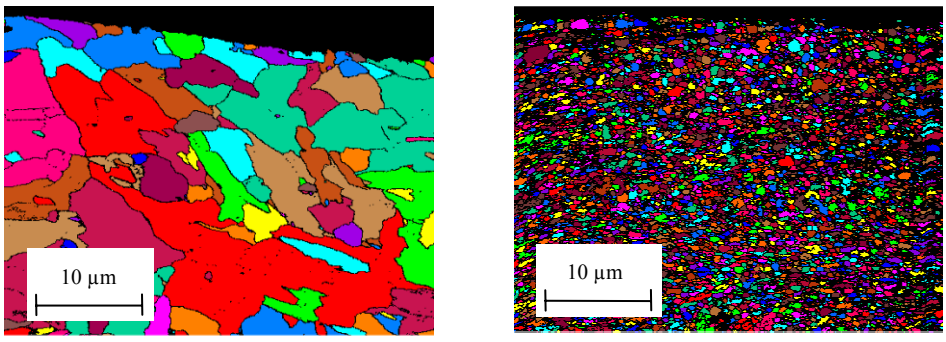

(a) AW (b) UIT

Fig. 11 Grain boundary images for the AW specimen and the UIT specimen.

The distribution of Vickers hardness (HV) from the surface to 2000 μm in depth at the weld toe was measured using a nanoindenter (FISCHERSCOPE HM2000). The nanoindenter measures the load and displacement of the indenter under loading and unloading conditions, and the Vickers hardness is calculated based on the relationship between the load and the displacement of the indenter[11]. The maximum load loaded to the indenter was 2000 mN. Figure 12 shows the distribution of the Vickers hardness for the AW specimen and the UIT specimen. The Vickers hardness on the surface was increased 1.3 times by the use of UIT. The depth to which hardness was increased by the use of UIT was from the surface to 300 μm in depth, which coincided with the depth of the grain refinement observed.

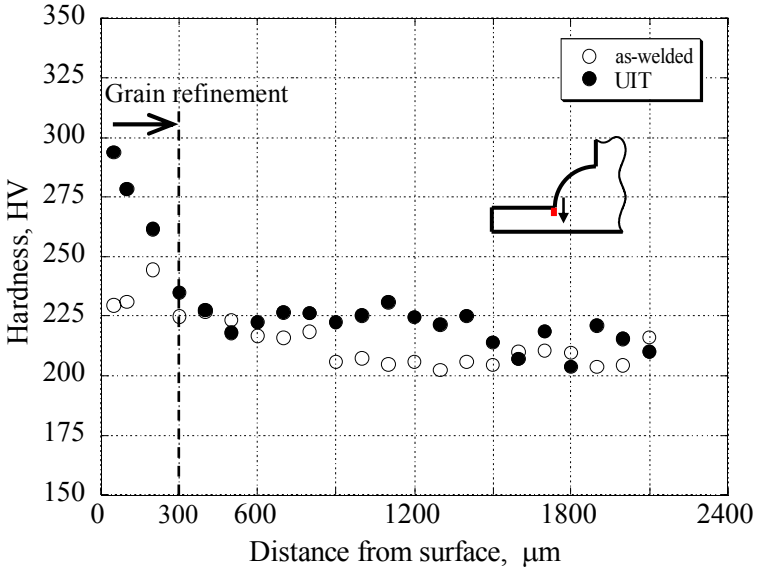

Fig. 12 Distribution of Vickers hardness.

4. Conclusions

In order to examine the effect of UIT on the fatigue lives of web-gusset welded joints, fatigue tests were carried out on joints that had been treated by UIT and the results were then compared with the results obtained for as-welded joints. Also, changes in the residual stress, stress concentration factor, and grain size around the weld toes resulting from the use of UIT were measured. The following conclusions were obtained.

(1) The fatigue lives of web-gusset welded joints treated by UIT were more than ten times those of as-welded joints, and the fatigue limit increased from 53 MPa to 111 MPa.

(2) The improvement in the fatigue lives as a result of the use of UIT was caused by an increase in the fatigue crack initiation life in the stress range of over 175 MPa. In the stress range of 175 MPa or less, the fatigue lives of the joints increased because the location at which fatigue cracks were initiated changed from the weld toe to the weld root.

(3) The residual stress on the surface at the weld toe changed from 300 MPa to −200 MPa after UIT was applied.

(4) The stress concentration factor at the weld toes in the UIT specimens calculated using FEM decreased by about 40% in comparison with that of AW specimens.

(5) The grain sizes under the weld toe in the UIT specimen was 0.3 to 0.7 μm, one-tenth or less the grain sizes in the AW specimen.

(6) The Vickers hardness at the weld toe in the UIT specimen increased from the surface to 300 μm in depth, which coincided with the depth of the grain refinement observed.

Acknowledgements

The application of UIT to the web-gusset welded joints used in this study was conducted at the Technical Development Bureau of Nippon Steel Cooperation. The authors would like to thank Dr. Tetsuro Nose and Dr. Hiroshi Shimanuki, both of whom work in the Technical Development Bureau, for all their help.

References

(1) Nakajima H., Nakamura H., and Suzuki H., Study on Fatigue Strength of Web-Gusset Welded Joints, *Journal of Constructional Steel*, Vol.14, (2006), pp.583-586.

(2) Ushirokawa O., and Nakayama E., Stress Concentration Factor at Welded Joints, *Ishikawajima Harima Engineering Review*, Vol.23, No.4, (1983), pp.351-355.

(3) Hasegawa M., Suzuki H., and Miura K., Effect of Strong Shot peening Cleaning and Hot Galvanizing on Fatigue Strength of Steel Welded Joint, *Quarterly Journal of the Japan Welding Society*, Vol.25, No.4, (2007), pp.486-493.

(4) Anami K., Miki C., Yamamoto H., and Higuchi Y., Fatigue Strength of Welded Joint Made of High Strength Steel and Fatigue Strength Improvement, *Journal of Structural Mechanics and Earthquake Engineering (I)*, No.675, (2001), pp.251-260.

(5) Hirayama S., Mori T., and Inomata T., Influence of Grinding Method on Fatigue Strength of Web-Gusset Welded Joints, *Steel Construction Engineering*, Vol.12, No.45, (2005), pp.111-121.

(6) Nose, T., Ultrasonic Peening Method for Fatigue Strength Improvement, *Journal of the Japan Welding Society*, Vol.77, No.3, (2008), pp.210-213.

(7) Nose, T., and Shimanuki, H., Experiment and Analysis of Influence of Ultrasonic Peening on Fatigue Life in Pad Welded Joint, *Transactions of the Japan Society of Mechanical Engineers, Series A*, Vol.74, No.737 (2008), pp.166-168.

(8) The Japan Society of Mechanical Engineers ed., *JSME STANDARD Standard Method of Statistical Fatigue Testing (2nd Edition) JSME S 002*, (1994), pp.8-15, The Japan Society of Mechanical Engineer.

(9) Machida S., Matoba M., Yoshinari H., Lin C., and Makino H., Consideration on Estimation of Welded Structure's Fatigue Life under Block Loading, *Journal of the Society of Naval Architects of Japan*, No.172, (1992), pp.579-587.

(10) Rigaku Corporation, *X-ray Diffraction Handbook* (in Japanese), (2006), pp103-104. Rigaku Corporation.

(11) Fischer, *Operating Instructions FISCHERSCOPE HM2000*, (2003), pp.97-102, Fischer.